International Journal of Applied Engineering Research ISSN 0973-4562 Volume 10, Number 18 (2015) pp 39522-39527

A Study on Structural and Thermal Durability for the Types of Brake Pad and Shoe

Jae Ung Cho[1]

[1] *Division of Mechanical & Automotive Engineering, Kongju National University, 1223-24, Cheonan Daero, Seobuk-gu, Cheonan-si, Chungnam, 31080, Korea*
E-mail: jucho@kongju.ac.kr

Abstract
In this study, simulations were conducted for brake pad and shoe, and analyses were performed for structure, heat transfer and thermal stresses. The shapes of models designed by using CATIA are analyzed with ANSYS program. To compare deformation and stress values due to thermal loads, structural analysis is carried out while each heat transfer analysis is conducted to find stresses due to heat. In terms of strength for structural analysis, i.e., whether large stresses can be withstood or not, the model of shoe type showed higher safety than two models of pad type. In the durability for vibration, two models of pad type can be seen to be higher than shoe type. In heat transfer and stress values due to heat, two models of pad type can be seen to be higher than shoe type.

Keywords: Durability, Brake Pad, Shoe, Thermal Stress, Thermal Deformation, Structural Analysis, Heat Transfer

Introduction

The pad in a disk brake system is a key safety part which safely decelerates or stops automobiles in driving or maintaining a parking condition by converting kinetic energy to thermal energy as braking hydraulic pressures, transmitted through a caliper, generate frictional resistance due to contacts between counterpart faces of the disk pad's frictional materials. Brake shoe also plays the same role as the pad. Brake shoe, is an arc-shaped part made of cast iron arranged in a brake drum and has a brake lining attached as a frictional material, which generates braking power through being pushed against the brake drum by hydraulic pressures imposed on the wheel cylinder; it returns automatically to its original position by a force of the return spring when hydraulic pressures are released[1-3]. While most of the previous vehicles had brake pads mounted on the front wheels and brake shoes on the rear wheels, all recent vehicles have a trend of the pad type being mounted of all wheels. Although passenger cars are primarily of the pad type, large-scale vehicles such as trucks are equipped with the shoe type due to structural problems, etc. Recently, as sizes, weights, driving speeds are increased due to speeding and high performance of vehicles, development aimed at improvement of reliability and durability is in progress for brake systems involving frictional materials[4-6].

This study will be able to find advantages and disadvantages of each through comparing two models by using the data values produced from analyses using the pad and the shoe models. If the results are combined for application to brake designs, modelling is considered possible by reviewing and predicting durabilities[7-12]. Pad and shoe models were modelled by using CATIA program. Each model was analyzed with ANSYS program. These models were analyzed by three types of analyses including structural analysis, heat transfer analysis and thermal stress analysis for extraction of data. Deformations and equivalent stresses are investigated by applying pad and shoe modeling with pressures and moments through structural analysis. Heat transfer analysis enables the application data for transfer of heat produced in frictional materials by using differences between the temperature of the brake in operation and the ambient temperature.

Study Model and Constraints

This study employs brake pad and shoe among automotive braking apparatuses as a model and analyzes by inputting data such as force, moment, temperature, etc. Each analysis per shape is conducted for the model prepared by employing CATIA program with the use of ANSYS program. To compare deformation and stress values due to thermal loads, a structural analysis is implemented, while heat transfer and thermal stress analyses are also conducted to find stresses due to heat. The material for the back plate of the pad and shoe was determined to be a structural steel, and material properties of the frictional material were used for the frictional face of pad and the brake lining. Actual models of model 1, model 2 and model 3 are shown in Figure 1. Also, mesh models of model 1, model 2 and model 3 are shown in Figure 2. The numbers of nodes and elements for the mesh of model 1 are 6508 and 3405, respectively, while those for the mesh of model 2 are 6755 and 2983, respectively, and those for the mesh of model 3 are 7867 and 3650, respectively. Material properties of the structural steel and the frictional material are shown in Table 1 and Table 2, respectively.

(a) Model 1

(b) Model 2

(c) Model 3

Figure 1: Actual configuration of models 1, 2 and 3

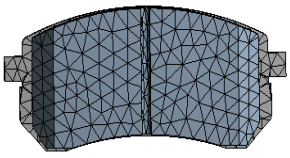

(a) Model 1

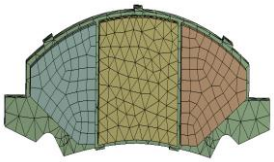

(b) Model 2

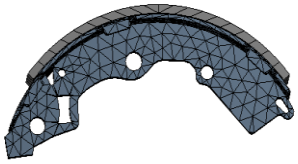

(c) Model 3

Figure 2: Meshes of models 1, 2 and 3

Table 1: Material properties of structural steel

Contents (Unit)	Value
Young's Modulus (MPa)	200000
Poisson's Ratio	0.3
Density (kg/m^3)	7850
Isotopic Thermal Conductivity(W/m°C)	60.5

Table 2: Material properties of frictional material

Contents (Unit)	Value
Young's Modulus (MPa)	9500
Poisson's Ratio	0.14
Density (kg/m^3)	2065
Isotropic Thermal Conductivity(W/m°C)	1.5

For boundary conditions required for analysis in this study, fixed conditions, forces and moments are needed. Boundary conditions for model 1, model 2 and model 3 are shown in Figure 3. While model 1 and model 2 had side faces of back plate fixed, shoe of model 3 had front, rear faces of the plate fixed. Also, pressures applied to the pad and the shoe may be seen. 0.25 MPa of force was applied to the rear face subjected to a force due to the hydraulic pressure inside a caliper. As in Figure 3, the moment due to rotation was given as 2500 $N \cdot mm$. On braking, when the brake pedal is stepped on the actual brake pad applies a counterforce on the rotating disc, with the friction that is produced by the contact of the horizontal length of the pad and the disc, the breaking moment is initiated, the braking force applied was found to be 25N.

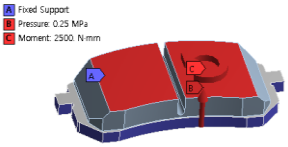

(a) Model 1

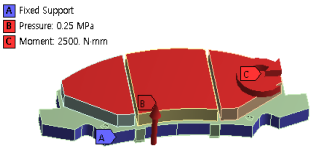

(b) Model 2

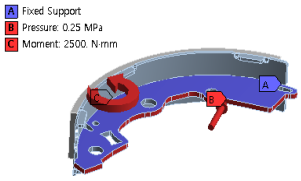

(c) Model 3

Figure 3: Boundary conditions for models 1, 2 and 3

Structural Analysis Result

Figure 4 shows contour lines of total deformation for each model. Maximum deformation of model 1 is shown to be 0.00040136mm, while that of model 2 is 0.00037405mm, and that of model 3 is 0.00021813mm. When the results are compared each other, model 1 could be seen to exhibit the largest deformation.

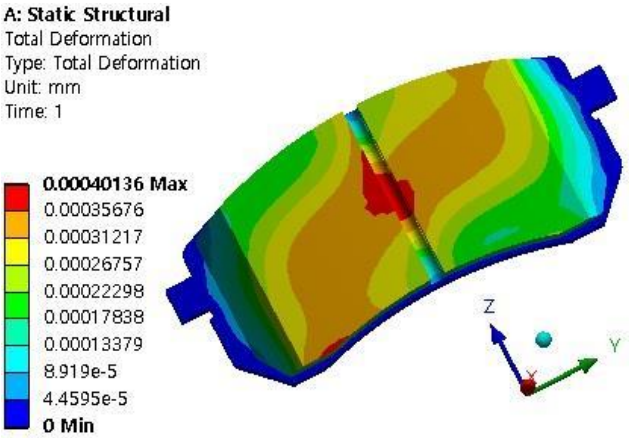

(a) Model 1

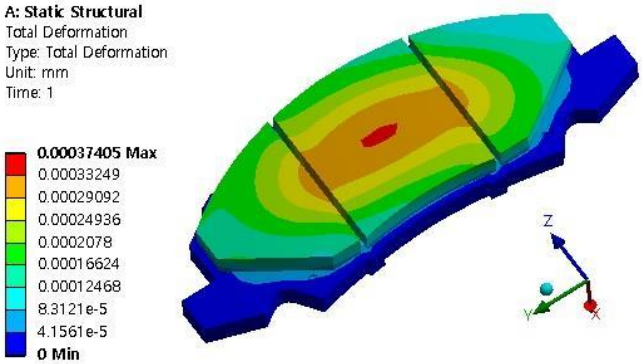

(b) Model 2

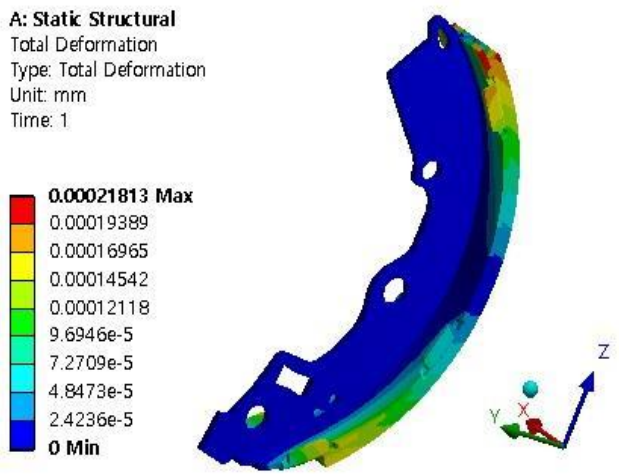

(c) Model 3

Figure 4: Contours of total deformations for various models

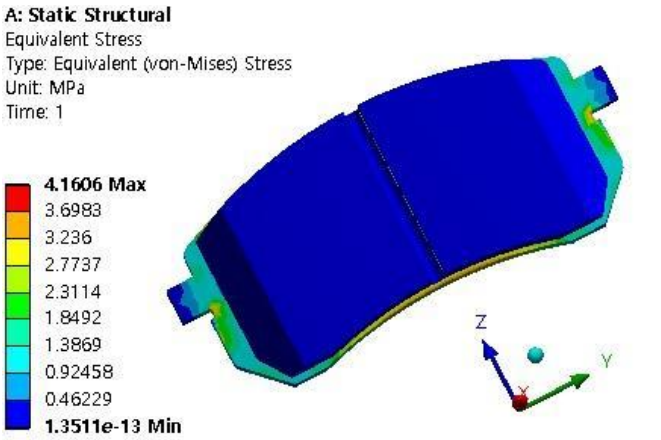

(a) Model 1

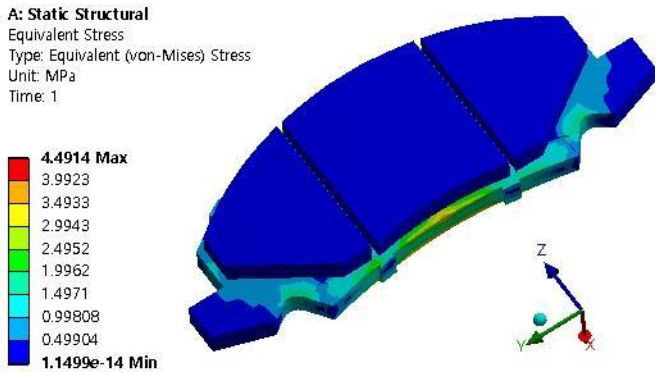

(b) Model 2

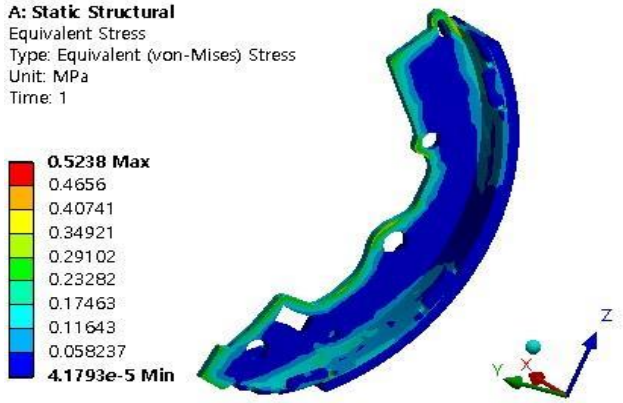

(c) Model 3

Figure 5: Contours of equivalent stresses for various models

According to Figure 5, the maximum equivalent stress of model 1 is shown to be 4.1606MPa, while that of model 2 is 4.4914MPa, and model 3 is 0.5238MPa. Comparison of the result values shows that the maximum equivalent stresses were largest in the order of models 2, 1, 3. Namely, model 3 shows the best strength for structural analysis.

Heat Transfer Analysis Result

Heat transfer involves a thermal energy which is moved by a temperature difference. Heat transfer always occurs whenever a temperature difference exists within a medium. In this study, the process where heat generated upon braking by pad and shoe was transferred through outside temperatures. Thermal conductivity of the frictional material was set to be 1.5 $W/m^{\circ}c$. The pad should be able to withstand thermal loads of about 750 $^{\circ}c$, up to about 950 $^{\circ}c$ instantaneously. For temperature conditions in the analysis, temperature of the frictional material upon braking was set to be 300 $^{\circ}c$ rather than an extreme condition, while outside temperature was set to be 22 $^{\circ}c$. Figure 6 shows boundary conditions for each model. The temperature of the face subjected to friction and the outside temperature were applied.

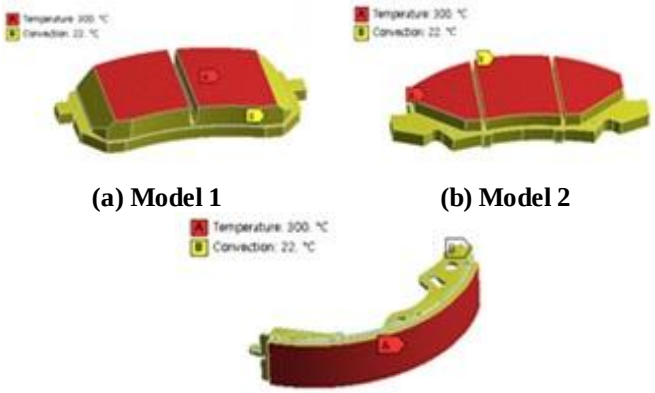

(a) Model 1 **(b) Model 2**

(c) Model 3

Figure 6: Boundary conditions for various models

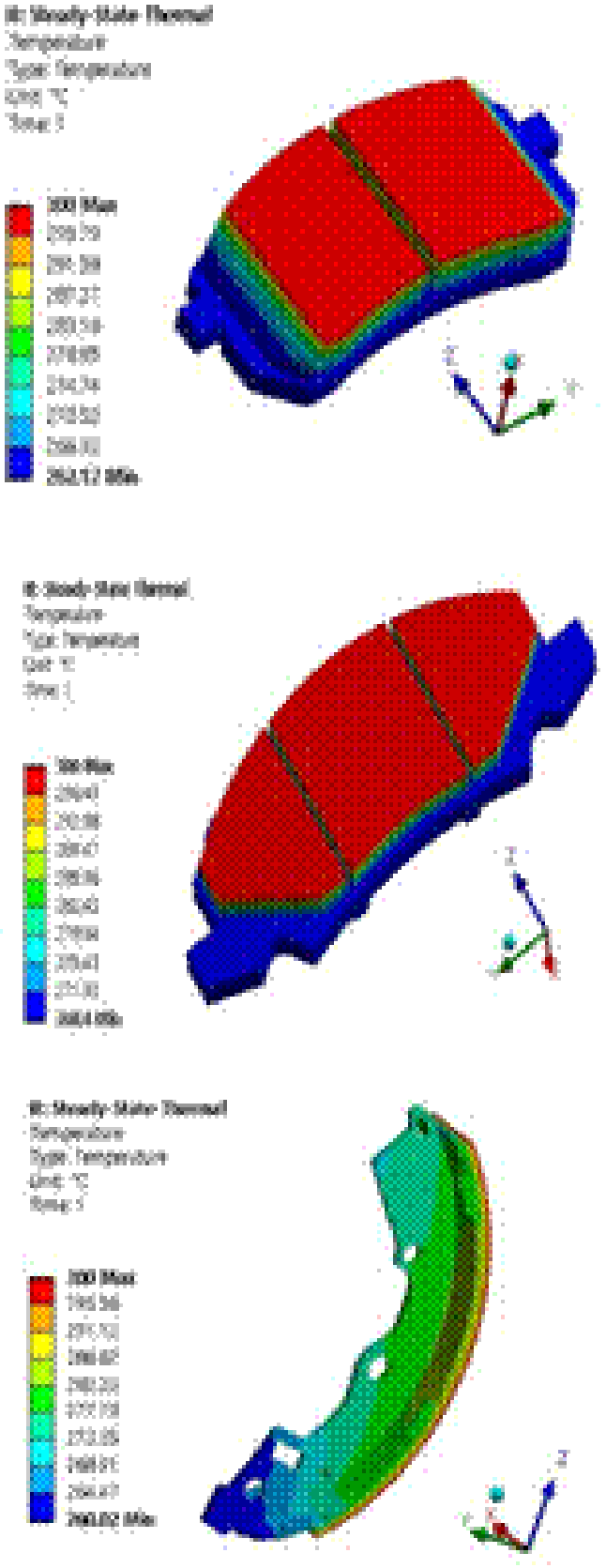

Figure 7: Thermal analyses for various models at steady state

According to the heat transfer analysis results, data of 262.16 $^{\circ}C$ for model 1, 268.40 $^{\circ}C$ for model 2, 260.02 $^{\circ}C$ for model 3 were obtained. When conditions were given for the temperature of the frictional material and outside temperature, appearance can be observed where heat in each model is transferred. model 2 with heat transfer up to 268.40 $^{\circ}C$ ~300 $^{\circ}C$ can be seen to show the best heat transfer, indicating more heat transfer than other models by about 7~9 $^{\circ}C$. Shapes of heat transfer about each model are seen in Figure 7.

In the process of heat transfer, stresses and deformations due to heat can occur. Thermal deformation is a special case of elastic deformation, the results of which appear when temperatures are raised for expansion or lowered for shrinkage. Such phenomenon shows a similar tendency in most isotropic materials. The fact that thermal deformation rate(ε) at a given temperature(T) is proportional to temperature changes (ΔT) within a limited range of temperatures may be expressed as follows.

$$\varepsilon = a(T - T_0) = a(\Delta T)$$

where T_0 is the initial temperature, and a is the thermal expansion coefficient. Since elastic deformation satisfies Hook's law where E is the elastic modulus, thermal stress σ is given as follows, with application of a convection transfer coefficient.

$$\sigma = Ea(\Delta T) = E\varepsilon$$

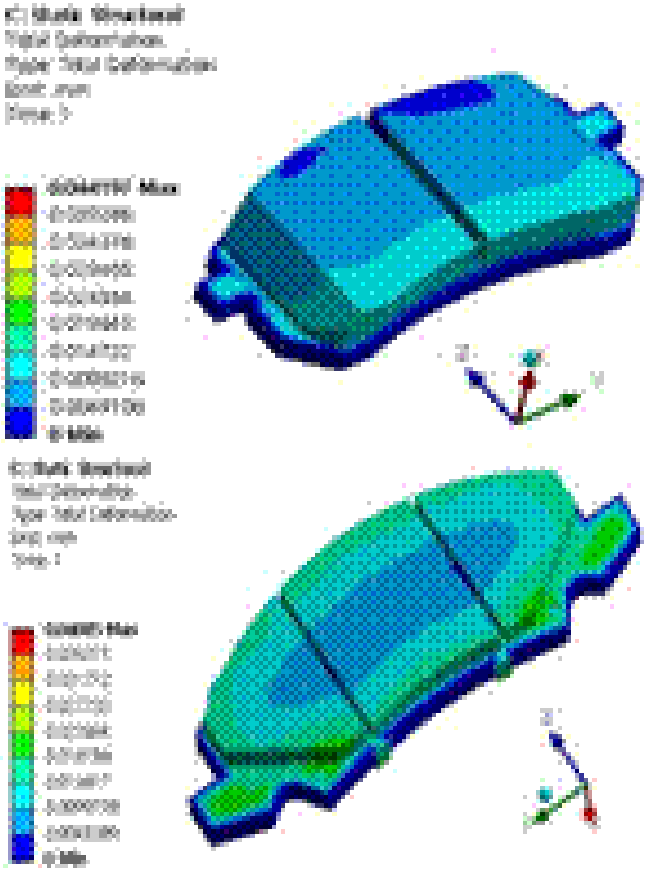

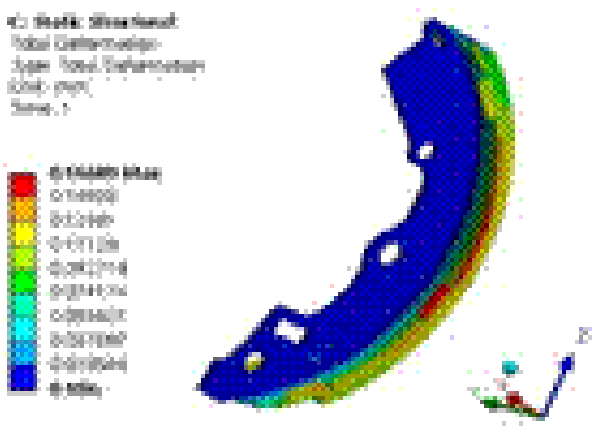

Figure 8: Thermal deformations in various models at steady state

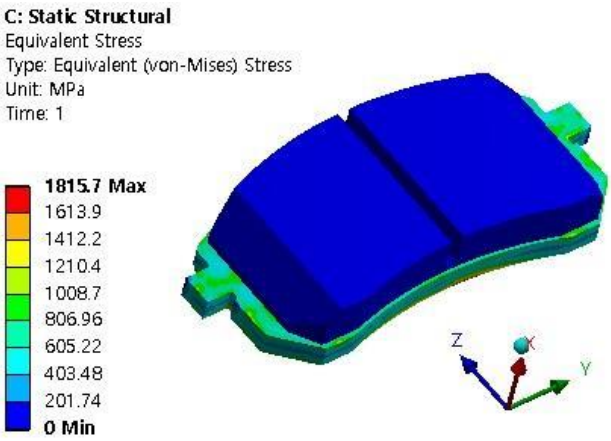

(a) Model 1

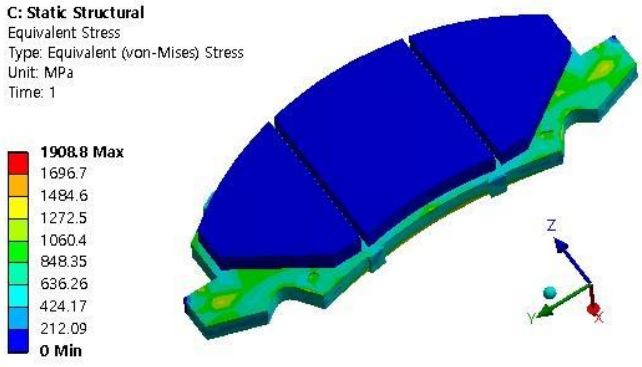

(b) Model 2

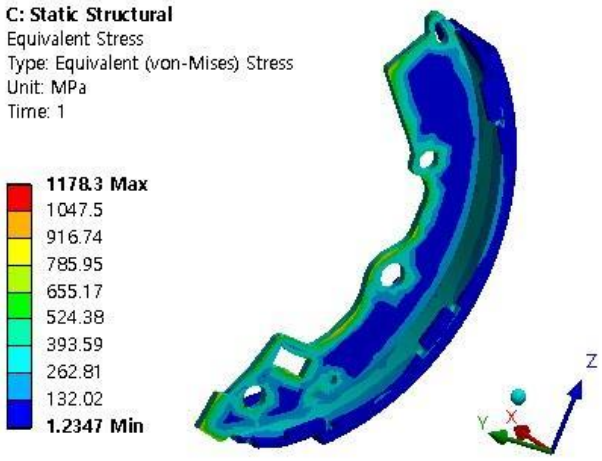

(c) Model 3

Figure 9: Thermal equivalent stresses in various models at steady state

In Figures 8 and 9, deformations and stresses due to heat can be seen. Considering the values of each model, deformation and thermal stress values due to heat for model 1 are shown to be 0.044197mm, 1815.7MPa, respectively, while those for model 2 are 0.04085mm, 1909.8MPa, respectively, and those for model 3 are 0.16687mm, 1178.3MPa, respectively. Maximum thermal stress values of each model are only an extremely small part, and there may be the possibility of failure. When the results are compared each other, the deformation due to heat is 0.1687mm for model 3, which represents the largest deformation while the largest stress value is 1909.8MPa for model 2.

Conclusions

In this study, simulations were conducted for brake pad and shoe, and analyses were performed for structure, heat transfer and thermal stresses.

According to the structural analysis, maximum equivalent stress for model 3 was 0.5238MPa which was smaller than those for models 1 and 2 by 8 times and 9 times, respectively. Model 3 has the best strength for structural analysis so that it is considered to be capable of withstanding larger loads than models 1 and 2. For the results of deformation due to forces and moments, all three types of models showed a value less than 0.0005mm with slight differences among them. The model showing the largest deformation was that of the pad at model 1 with a value of 0.0004mm.

As a result of heat transfer, model 2 showed transfer of heat up to 268.4 $^{\circ}C$ ~300 $^{\circ}C$, indicating more heat transfer than other models by about 7~9 $^{\circ}C$. In terms of the maximum thermal deformation, model 3 showed the largest deformation of 0.16687mm. Also, in thermal stresses, model 2 showed the highest stress value of 1909.8MPa.

In terms of strength for structural analysis, i.e., whether large stresses can be withstood or not, the model of shoe type showed higher safety than two models of pad type. In durability for vibration, two models of pad types can be seen to be higher than the model of shoe type. In heat transfer and stress values

due to heat, two models of pad types can be seen to be higher than the model of shoe type. Heat transfer analysis in this study enables the application data for transfer of heat produced in frictional materials by using differences between the temperature of the brake in operation and the ambient temperature.

References

[1] Werner, Ö., and Ingrid U., 2006, "Third body formation on brake pads and rotors," Tribology International, 39(5), pp. 401-408.

[2] Michal, K., 2011, "The thermal problem of friction during braking for a three-element tribosystem with a composite pad," International Communications in Heat and Mass Transfer, 38(10), pp. 1322-1329.

[3] Palhade, R. D., Tungikar, V. B., Dhole, G. M., and Kherde, S. M., 2013, "Transient Thermal Conduction Analysis of High Voltage Cap and Pin Type Ceramic Disc Insulator Assembly," IJAST, 56, pp.73-86.

[4] Tomas U. G. Jr., 2013, "Investigation on the use of Coco Coir Polypropylene as Thermal Insulator," IJAST, 59, pp.13-26.

[5] Karimi, and G., Culham, J. R., 2002, "Thermal comfort analysis of an automobile driver with heated and ventilated automotive seat," SAE 2002-01-0222.

[6] Huang, D. S., and Huang, F. C., 2014, "Coupled thermo-fluid stress analysis of Kambara Reactor with various anchors in the stirring of molten iron at extremely high temperatures," Applied Thermal Engineering, 73(1), pp. 220-226.

[7] Laroussi, M, Djebbi, M, and Moussa, M., 2014, "Triggering vortex shedding for flow past circular cylinder by acting on initial conditions: A numerical study," Computers and Fluids, 101(20), pp.194-207.

[8] Emma, F., Adolfo, S., Dario, B., and Mario, U. M., Micaela, O., 2014, "A tridimensional CFD analysis of the oil pump of an high performance motorbike engine," Energy Procedia, 45, pp. 938-948.

[9] Karimi, G., Chan E. C., and Culham, J. R., 2002, "Thermal Comfort Analysis of an Automobile Driver with Heated and Ventilated Automotive seat," SAE 2002-01-0222.

[10] Ferreira, M. A., and Tribess, A., 2009, "User' Perception of Thermal Comfort in Ventilated Automotive Seat," SAE 2009-36-004.

[11] Rashed, A. N. Z., 2012, "Harmful Effects of Gamma Irradiation on Optical Fiber Communication System Links under Thermal Environment Effects," IJAST, 41, pp. 1-14.

[12] Cho, J. U., 2015, "Analyses of Structure and Heat Transfer for Brake Pad and Shoe Models," Advanced Science and Technology Letters, 108, pp. 19-23.